



NRC Publications Archive Archives des publications du CNRC

Accelerated durability testing via reactants relative humidity cycling on PEM fuel cells

Panha, Karachakorn; Fowler, Michael; Yuan, Xiao-Zi; wang, Haijiang

This publication could be one of several versions: author's original, accepted manuscript or the publisher's version. / La version de cette publication peut être l'une des suivantes : la version prépublication de l'auteur, la version acceptée du manuscrit ou la version de l'éditeur.

For the publisher's version, please access the DOI link below. / Pour consulter la version de l'éditeur, utilisez le lien DOI ci-dessous.

Publisher's version / Version de l'éditeur:

<https://doi.org/10.1016/j.apenergy.2011.05.011>

Applied Energy, 93, pp. 90-97, 2011-06-02

NRC Publications Record / Notice d'Archives des publications de CNRC:

<https://nrc-publications.canada.ca/eng/view/object/?id=32998ad6-fb43-4ef9-a14e-2623570b89d5>

<https://publications-cnrc.canada.ca/fra/voir/objet/?id=32998ad6-fb43-4ef9-a14e-2623570b89d5>

Access and use of this website and the material on it are subject to the Terms and Conditions set forth at

<https://nrc-publications.canada.ca/eng/copyright>

READ THESE TERMS AND CONDITIONS CAREFULLY BEFORE USING THIS WEBSITE.

L'accès à ce site Web et l'utilisation de son contenu sont assujettis aux conditions présentées dans le site

<https://publications-cnrc.canada.ca/fra/droits>

LISEZ CES CONDITIONS ATTENTIVEMENT AVANT D'UTILISER CE SITE WEB.

Questions? Contact the NRC Publications Archive team at

PublicationsArchive-ArchivesPublications@nrc-cnrc.gc.ca. If you wish to email the authors directly, please see the first page of the publication for their contact information.

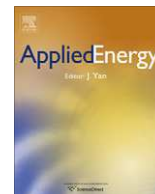
Vous avez des questions? Nous pouvons vous aider. Pour communiquer directement avec un auteur, consultez la première page de la revue dans laquelle son article a été publié afin de trouver ses coordonnées. Si vous n'arrivez pas à les repérer, communiquez avec nous à PublicationsArchive-ArchivesPublications@nrc-cnrc.gc.ca.





Contents lists available at ScienceDirect

Applied Energy

journal homepage: www.elsevier.com/locate/apenergy

Accelerated durability testing via reactants relative humidity cycling on PEM fuel cells

Karachakorn Panha^a, Michael Fowler^{a,*}, Xiao-Zi Yuan^b, Haijiang Wang^b

^a Department of Chemical Engineering, University of Waterloo, 200 University Avenue West, Waterloo, ON, Canada N2L 3G1

^b NRC Institute for Fuel Cell Innovation, 4250 Wesbrook Mall, Vancouver, BC, Canada V6T 1W5

ARTICLE INFO

Article history:

Received 29 September 2010

Received in revised form 20 April 2011

Accepted 4 May 2011

Available online xxxxx

Keywords:

Relative humidity (RH)

Accelerated durability testing

Degradation mechanisms

Linear sweep voltammetry (LSV)

Hydrogen crossover current

Fluoride ion release concentration

ABSTRACT

Cycling of relative humidity (RH) levels in polymer electrolyte membrane (PEM) fuel cells reactant streams have been reported to decay fuel cell performance. This study focuses on accelerated durability testing to examine different modes of membrane failure via relative humidity cycling. A single fuel cell with an active area of 42.25 cm² was tested. A Hydrogenics G50 test station was used to establish baseline cell with 840 h of degradation under high humidity idle conditions at a constant current density of 10 mA cm⁻². The membrane electrode assembly (MEA) contained a Gore™ 57 catalyst coated membrane (CCM) and 35 BC SGL gas diffusion layers (GDLs). During the test, in situ diagnostic methods, including polarization curves and linear sweep voltammetry (LSV) were employed. Also, ex situ tests such as ion chromatography, infrared imaging, and scanning electron microscopy were used to identify degradation mechanisms. For RH cycling cell, H₂–air inlet gases were alternated under dry and 100% humidified conditions every 10 and 40 min, respectively. Under idle conditions, operated at very low current density, a low chemical degradation rate and minimal electrical load stress were anticipated. However, the membrane was expected to degrade due to additional stress from the membrane swelling/contraction cycle controlled by RH. The degradation rate for steady state conditions (0.18 mV h⁻¹) was found to be lower than under RH cycling conditions (0.24 mV h⁻¹). Change in RH led to an overall PEM fuel cell degradation due to the increase in hydrogen crossover current and fluoride ion release concentration. This study advanced the development of 'diagnostics' for PEM fuel cells in that failure modes have been correlated with in situ performance observations.

© 2011 Elsevier Ltd. All rights reserved.

1. Introduction

Polymer electrolyte membrane (PEM) fuel cells are electrochemical devices that involve the electrochemical reaction of hydrogen and oxygen to produce electricity and water [1]. They are environmentally friendly energy producers that improve energy production by producing power more efficiently without any harmful emissions. PEM fuel cells are thus one of the leading clean energy technologies being considered for transportation applications and power generation [2]. One of the most important issues in the development of PEM fuel cells is membrane durability [3,4]. PEM fuel cells use a perfluorosulfonic acid (PFSA)/PTFE copolymer (e.g. Nafion™) membrane as an electrolyte to transport hydrogen ions from anode to cathode. Since the ions can only conduct at a desired rate when the membrane is hydrated, fuel cells typically operate with humidified gases, mainly H₂ and air at the anode and cathode, respectively [5,6].

The requirement for hydration of electrolyte membrane means that relative humidity (RH) levels of the reactant stream therefore have effects on PEM fuel cell performance. Reducing RH limits the electrode kinetic reactions and increases the membrane resistance inside the fuel cell [6]. Proton conductivity of the membrane and performance of the fuel cell will rapidly decrease when the water content of the membrane decreases, especially if operated with dry reactant gases [7,8]. On the other hand, water is produced in a PEM fuel cell, and at high current densities water has the potential to fill pores in the gas diffusion layer and inhibit mass transfer. Contact with liquid water can 'swell' the polymeric membrane, and thus change in hydration levels in the membrane can create mechanical stresses. Therefore, water management within a fuel cell is a complex phenomenon that must be carefully managed.

Recently, several studies have examined the degradation mechanism of the PEM in a membrane electrode assembly (MEA) under low humidification conditions [6,9,10]. Some researchers have focused on operating a PEM fuel cell with completely dry reactant gases, finding operation under such conditions feasible [7,11,12]. With a higher current density, more water is produced on the

* Corresponding author.

E-mail address: mfowler@uwaterloo.ca (M. Fowler).

cathode side and the water back-diffusion effect (water moving from cathode to anode) prevails over the electro-osmotic effect (water moving from anode to cathode), so the cell can be sufficiently humidified to continue and complete the necessary electrochemical reactions. However, at low current densities, both water back-diffusion and electro-osmotic effects are limited, indicating that the electrolyte membrane might not be sufficiently humidified for the ions to pass through it [4,13–16]. Because the conductivity of the membrane depends on its water content, RH is one of the important factors potentially affecting PEM fuel cell performance.

Fuel cells in certain applications (e.g. automotive) can be subjected to frequent start-stop cycles, prolonged idle conditions, and frequent current cycling due to variation in the demand of power from the overall power demand cycle [1]. RH cycling operating test has become an interesting accelerated test to study the PEM durability of the fuel cell. In this work, accelerated durability testing to study different modes of membrane failure via RH cycling under idle conditions is performed. Under the idle conditions, operating at very low current density, a low chemical degradation rate and minimal electrical load stress are anticipated. Note that both open circuit conditions [17] and high current density operation have been shown to be associated with accelerated chemical degradation of the membrane. However, the membrane was expected to degrade due to additional stress from the membrane swelling/contraction cycle controlled by the RH.

2. Experimental

Fuel cell experiments were conducted using a single TP50 fuel cell (Tandem Technologies) with an active area of 42.25 cm². The graphite plates contained serpentine path flow channels. The flow channels of the cathode and the anode plates differed in that those of the former were wider and deeper than those of the latter to increase the cross-sectional area for reactant diffusion.

Gore™ 57 catalyst coated membrane (CCM) with an overall thickness of 50 μm and a membrane thickness of 25 μm were used. The catalyst loading for both sides was 0.4 mg cm⁻². The MEA was assembled using a 150 μm Kapton gasket with the membrane sandwiched in the middle and 35 BC SGL gas diffusion layers (GDLs) were placed on either side. The TP50 fuel cell and a G50 test station were used to investigate RH effects on PEM fuel cell performance. Hydrogen and air were supplied as reactant gases to the anode and cathode sides, respectively. The gas lines to both sides were also connected to a nitrogen tank, allowing the system to be purged with nitrogen gas during electroanalytical testing (i.e., linear sweep voltammetry (LSV)). The fuel cell hardware was first compressed using nitrogen gas at 100 psig. Next, a water bath was used to heat the fuel cell to 70 °C and maintained that temperature. The reactant gases flowed through Bronkhorst EL-flow meters and pressure transducers before entering the humidifiers. External humidifiers were used in this system to keep the gas streams hydrated before entering the fuel cell so that the flowing gases would not dry out the MEA. A LabView control system and TDI load box were used to control the load. At the outlets, the gases left the fuel cell carrying the water generated. Product water was collected in the condensers and then further used for fluoride ion release analysis.

Idle conditions at a constant current density of 10 mA cm⁻² were employed for this work. Idle conditions were selected in order to minimize the chemical degradation associated with radical attack at open circuit voltage (OCV). Although the confounding effect of chemical degradation and catalyst degradation cannot be

completely eliminated the 'idle' conditions are the least stressful for these modes of aging. The test station was first used to perform a baseline cell under high RH (Run 1: 100% RH). The fuel cell was run at 70 °C with either at constant 0.113 slpm and 0.358 slpm or stoichiometric flow rates at the stoichiometric ratio of 1.5 and 2.5 for hydrogen gas and air, respectively. An external modification was made to the experimental set-up so that the test station humidification system was completely by-passed during the cycling, and completely dry reactants could be directly fed to the fuel cell. This allowed for rapid (almost immediate) and complete cycling between RH = 0 and RH = 100 (and the humidification system in the G50 could remain at steady state for return to operation). The hydrogen gas and in-house air were both set at 100 psig. At the beginning of the cell's life, commissioning processes were carried out, including leak testing, crossover testing, and break-in of the fuel cell. Commissioning was conducted to ensure the cell had no leaks and to allow the cell to warm up and become fully hydrated in order for the reactions to occur. In the RH cycling cell (Run 2), the same conditions were applied. However, instead of the reactant gases passing through the humidifiers before entering the fuel cell, the gases were supplied directly to the cell. The test station was by-passed to enable dry gas passage using additional valves at both anode and cathode sides. The by-pass configuration ensured that the RH of the inlet stream changed rapidly. In this case, the commissioning procedure was conducted for 120 h. During RH cycling, the inlet gases were automatically alternated between dry and 100% humidified conditions every 10 and 40 min, respectively. A schematic design of the RH alternation during H₂-air RH cycling is shown in Fig. 1. This cycling routine was experimentally determined in order to allow the cell to completely return to steady set prior to the next 'dry cycle', and then the duration of the 'dry cycle' was selected so that the cell performance was allowed to degrade without complete loss of performance.

In situ diagnostic methods, including polarization curves and LSV, were conducted to observe the degradation mechanisms. The current measured during LSV is known as the hydrogen crossover current. Crossover current measurements were performed by scanning the voltage from 0.05 to 0.6 V at a sweep rate of 2 mV s⁻¹. Electrochemical measurements were taken using EG&G Princeton Applied Research potentiostat/galvanostat Model 273 and Coreware software. In addition, ex situ tests, including ion chromatography, infrared (IR) imaging, and scanning electron microscopy (SEM) were conducted. Dionex ED40 electrochemical detector working with Dionex GP40 gradient pump was used to measure the fluoride ion release concentration arising from degradation of the membrane structure. Also, by using IR camera (InfraTech

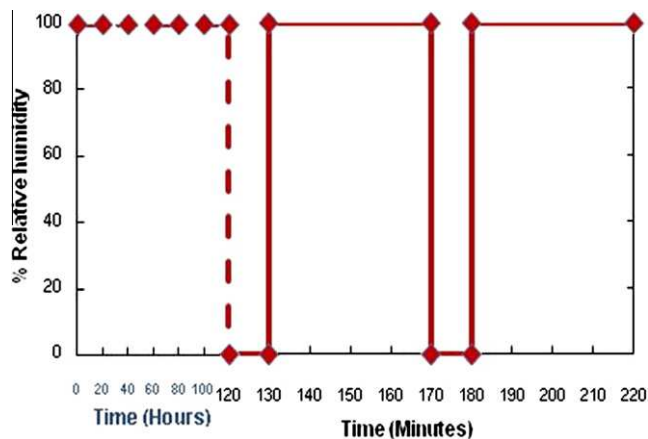


Fig. 1. Schematic design of the RH alternation during H₂-air RH cycling.

GmbH), IR imaging was performed. The IR images can distinguish the level of temperature distribution to observe hot spot/pin-hole formations of the degraded MEAs. Moreover, the SEM analysis is carried out using a LEO SEM with field emission Gemini Column to characterize the morphology and the change in thickness of the MEA samples.

3. Results and discussion

In this study, two fuel cells were operated under idle conditions. The first cell received fully humidified reactant gases and the second cell received H_2 -air cycled alternately between dry and humidified conditions at a constant current density of 10 mA cm^{-2} . The results of the RH effect on PEM fuel cell performance are summarized as follows:

3.1. RH effect on PEM fuel cell performance

Polarization curves of the two fuel cells at 70°C without backpressure are shown in Fig. 2a and b. Changes in polarization curves can indicate what material characteristics have been degraded [18]. A curve can be segmented into four regions – open circuit voltage (OCV), activation loss, linear ohmic loss, and mass transfer limitation – each characterized by a drop from the ideal Nernst po-

tential. The effects on these different regions indicate a decrease in a fuel cell's voltage output. In Fig. 2a, the 100% RH cell has a lifetime of 840 h. At 456 h there is an obvious change in the slope of the curve, which might have been caused by ionic capacity loss, membrane aging, hydrogen crossover, or early mass transfer limitation. In the case of the H_2 -air RH cycling cell, 130 cycles were completed over a cell lifespan of 622 h (Fig. 2b). RH cycling began after 120 h of commissioning. The curve starts to deviate from the original trend at 312 h. There is also a voltage dip at the higher current densities, which is thought to be the result of incipient mass transfer limitation inside the cell.

Fig. 2a and b also compare variations in cell voltages with current density for both cells operated at a constant current density of 10 mA cm^{-2} . The 100% RH cell shows a higher cell voltage output than the H_2 -air RH cycling cell. For example, at 312 h and a current density of 300 mA cm^{-2} , the cell voltages are 0.60 V (100% RH) and 0.52 V (RH cycling). Note that the period between polarization curves is not consistent due to equipment operation constraints. Also equipment and humidification variability resulted in some slight anomalies in the data (e.g. slightly higher performance at high current densities between curves for Run 696 h in Run 1 – Fig. 2a where the cell was not allowed to fully come to steady state operation). These do not significantly alter the observed trends.

Fig. 3a and b shows voltage degradation curves for both 100% RH and RH cycling cells, plotting potential at a constant current

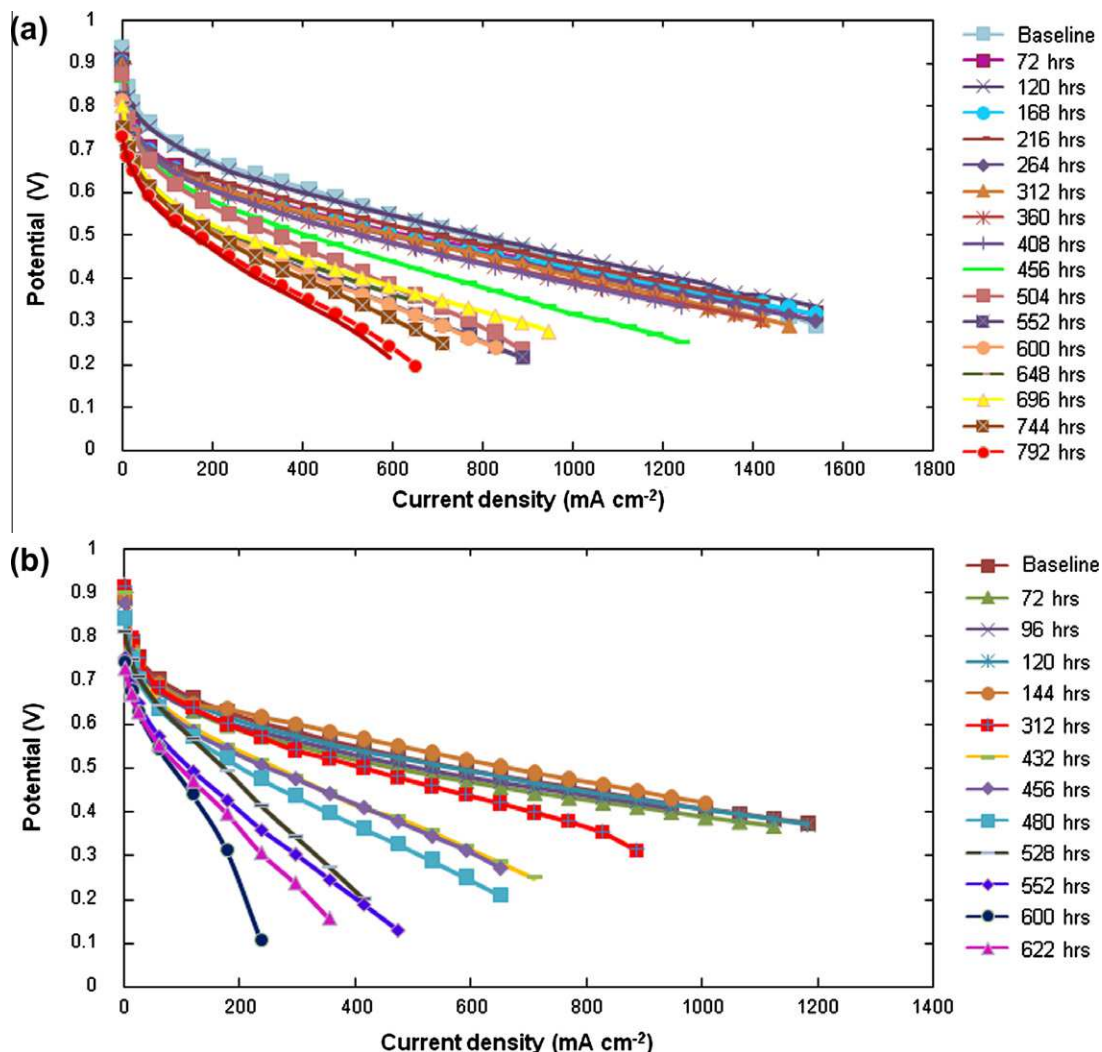


Fig. 2. PEM fuel cell polarization curves of (a) Run 1: 100% RH cell and (b) Run 2: H_2 -air RH cycling cell. The cells were operated at 70°C and a constant current density of 10 mA cm^{-2} without backpressure. MEAs active area: 42.25 cm^2 ; hydrogen and air flow rates: 0.113 and 0.358 slpm, respectively.

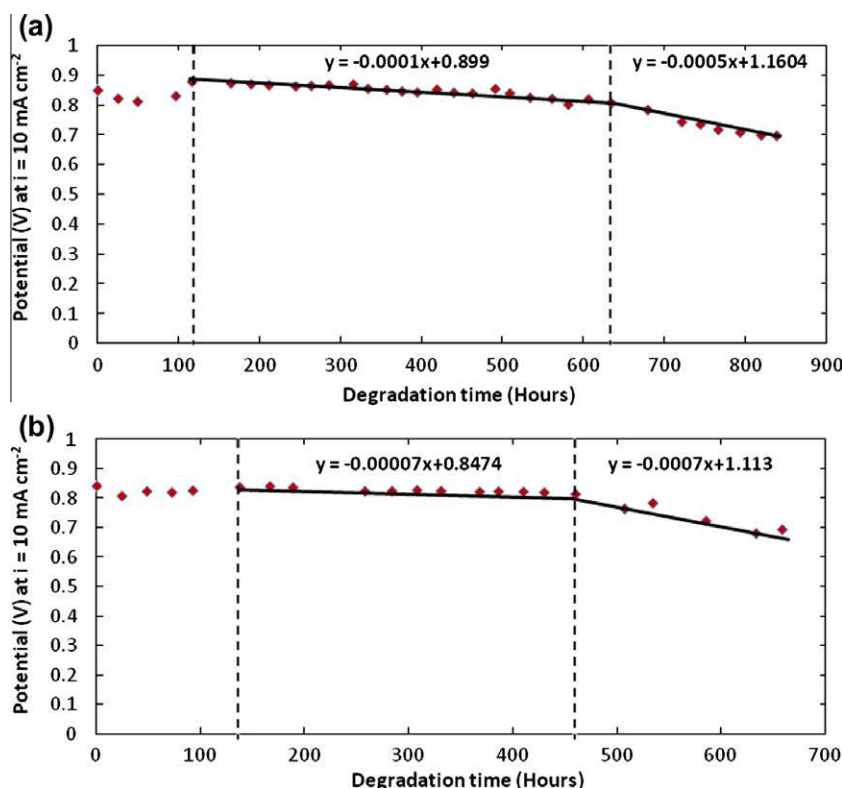


Fig. 3. Voltage degradation curves of (a) Run 1: 100% RH cell and (b) Run 2: H₂–air RH cycling cell. The cells were operated at 70 °C and a constant current density of 10 mA cm^{−2} without backpressure. MEAs active area: 42.25 cm²; hydrogen and air flow rates: 0.113 and 0.358 slpm, respectively.

density of 10 mA cm^{−2} versus degradation time. Both cells show quite a similar change in cell voltage: it increases somewhat during the commissioning procedure (0–120 h) and then slowly drops along the trend line. At approximately 620 h for the 100% RH cell and 450 h for the RH cycling cell, the voltages start to deviate from the original trend and drop below 0.8 V. As calculated from Fig. 3a and b, the overall cell degradation rates are 0.18 mV h^{−1} (100% RH) and 0.24 mV h^{−1} (RH cycling), respectively.

From the results of the polarization curves and the voltage degradation curves, the RH cycling cell clearly experienced a higher cell voltage degradation rate than the fully humidified cell. Both cells show a specific diagnostic feature where the slope of degradation curve changes later in life 100–200 h prior to cell failure.

3.2. RH effect as observed by hydrogen crossover current

Using LSV measurements, the hydrogen crossover currents of both cells (Run 1: 100% RH; Run 2: RH cycling) are compared in Fig. 4. The crossover current of the 100% RH cell gradually increases until 400 h and then the increase accelerates to reach 10 mA cm^{−2}, which indicates membrane failure [17]. The RH cycling cell's crossover current starts to increase after 200 h and exceeds 10 mA cm^{−2} at approximately 460 h. Note that the sharp rise in crossover during Run 2 does correlate in time (at about 460 h) with the diagnostic feature in the degradation curve, and a similar (although less distinctive) feature is observed in Run 1 at about 640 h.

During Run 2 with the RH cycling clearly membrane integrity was compromised at about 450 h of operation. Variation in RH can alter the hydrogen crossover current because crossover is a function of hydration and temperature [17]. RH also influences reactant partial pressures, membrane permeability, and membrane thickness [8]. During RH cycling, a change in reactant partial pressures can drive the gases to cross over from one side of the fuel cell

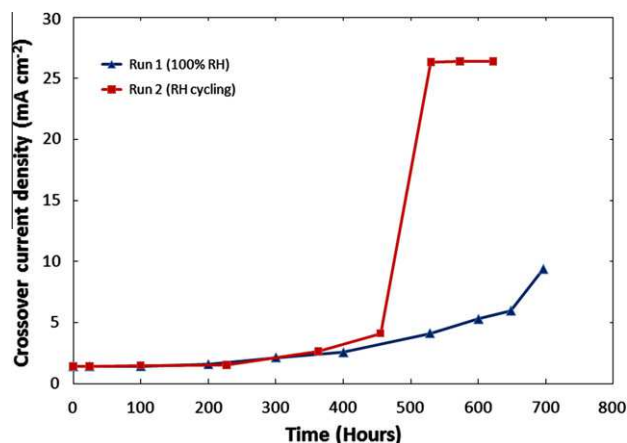


Fig. 4. Hydrogen crossover current densities of Run 1: 100% RH cell (triangles), and Run 2: H₂–air RH cycling cell (squares).

to the other. Partial pressure differentials in the reactants can also create localized stress on the membrane, leading to gas crossover. In addition, the membrane's permeability to the reactant gases typically increases along with RH which will increase either hydrogen or oxygen concentration [11–13]. Thus, it is believed that the crossover current through the membrane might increase by the effects of reactants changing from dry to fully humidified. As time passes, the electrolyte membrane is degraded and consumed, resulting in membrane thinning that allows the gases to easily cross over to either side. The combined RH effects are thought to lead to increased crossover, rips and tears in the membrane, and pinhole formation. Once pinholes arise, the crossover rate increases rapidly [10,19–21].

3.3. RH effect as observed by fluoride ion release

Fluoride ion release is a good indicator of overall membrane degradation [23,24]. The membrane degradation mechanism is believed to be loss of material as the membrane's polymeric structure deteriorates. When a PFSA membrane degrades, it releases peroxides and hydrogen fluoride (HF). Over the cell's operation time, these acidic byproducts can also degrade the cell components and cause failures such as cracks or pinholes. If such failures develop, leakage and crossover may increase, thereby degrading the fuel cell's performance and shortening its lifespan [23–26]. However, the integrity failure seen in other tests was not indicated in this diagnostic, which indicated that failure in this case is more predominately due to mechanical rather than chemical failure modes.

In the present study, effluent water from anode and cathode sides was collected during fuel cell operation. Ion chromatography was then used to measure the fluoride ion concentration arising from degradation of the membrane structure. By measuring the total amount of water produced, the fluoride ion release rate and the cumulative amount of released fluoride ions could be determined.

Fig. 5a and b present fluoride ion release rate as a function of time. The rates peak at approximately 150 h for both cells, which agrees with results reported by Kundu et al. [23] and Liu et al. [26] using Gore™ membranes. After RH cycling starts, some points show a higher fluoride release rate at the anode side than at the cathode side (Fig. 5b, Run 2: H₂–air RH cycling). This is thought

to be due to the change in RH that occurs when the difference between the reactants' partial pressures increases. Variation in RH should alter the water drag characteristics between the anode/cathode interfaces. Alternating the water drag characteristics increases anodic fluoride release and decreases cathodic fluoride release [7,5,9,11].

The cumulative fluoride ion releases of the two runs are compared in Fig. 6. All the curves seem to trace an exponential rise at the beginning, changing to a linear increase and reaching an upper limit at the end. The RH cycling cell shows a higher cumulative fluoride ion release on both anode and cathode curves than the fully humidified cell. For instance, at 200 h, the cumulative fluoride ion releases are 2 $\mu\text{mol cm}^{-2}$ (100% RH) and 9 $\mu\text{mol cm}^{-2}$ (RH cycling) for the anodes, and 6 $\mu\text{mol cm}^{-2}$ (100% RH) and 17 $\mu\text{mol cm}^{-2}$ (RH cycling) for the cathodes. As these figures indicate, both cells have a high cumulative fluoride ion release at the cathode side, which is believed to be due to the change in water drag inside the cell and the degradation occurring close to the cathode catalyst/ionomer interface [5,22,23].

3.4. RH effect as observed by infrared (IR) imaging

By using IR camera (InfraTech GmbH), IR imaging was performed. The IR images can distinguish the level of temperature distribution between fresh and degraded MEAs of each run. Variation in temperature distribution is thought to be due to the change in the level of reactant crossover through the MEA. As the reactant crossover increases, more heat is generated resulting in higher temperature distribution on the MEA [27]. To diagnose MEA degradation, the temperature distribution through IR images is then used for comparing the RH effect of Run 1 and Run 2.

After running approximately for 650 h, Run 1 was dismantled for IR imaging. Two different hydrogen concentrations were used for this run. Pure hydrogen was first provided by flowing in the top right side of the MEA image at 5 psi and 30 ml min⁻¹. Fig. 7a and b shows the IR images of fresh and degraded MEAs under H₂–air fully humidified. It can be seen that the maximum temperature of the degraded sample is about 2 °C higher than the fresh sample. The decayed sample shows some hot spots that generate close to the cathode outlet in the particular area. At the end of cell's life (840 h), the temperature distribution on the MEA was observed by using 20% H₂ in N₂. In this case, diluted hydrogen was used to avoid burning of the degraded sample. The hydrogen was fed at the top right side of the MEA with the same rate and pressure. From Fig. 7d the IR image clearly shows a new hot spot occurring at the bottom right side of the image which is believed to be close

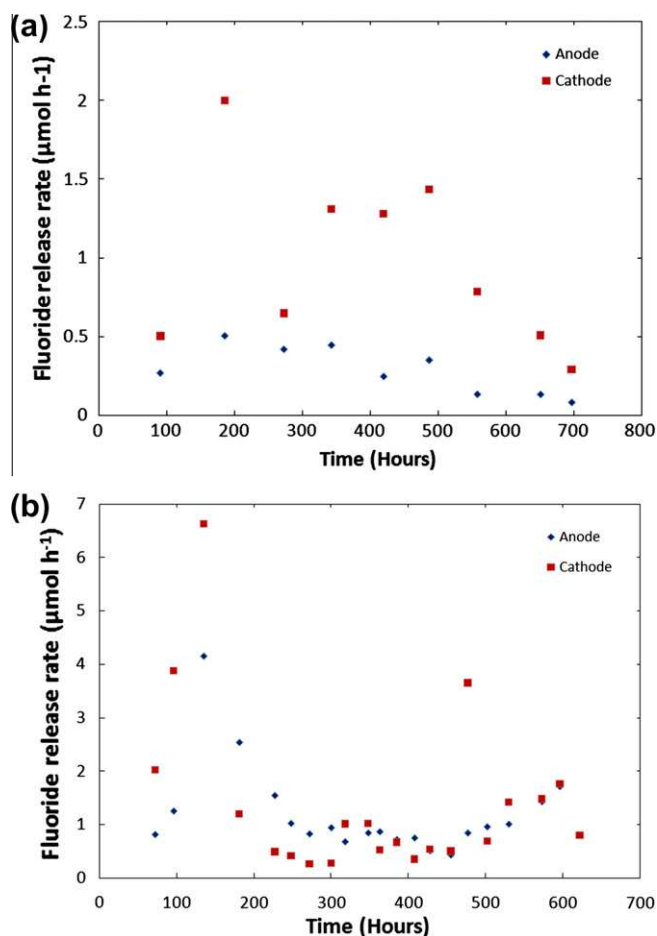


Fig. 5. Fluoride ion release rates of (a) Run 1: 100% RH cell, and (b) Run 2: H₂–air RH cycling cell.

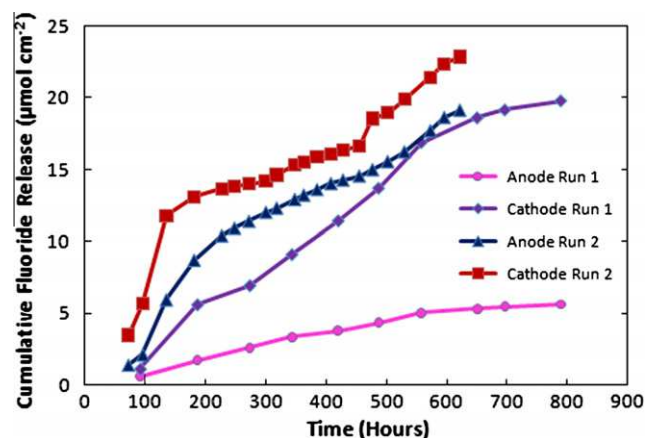


Fig. 6. Cumulative fluoride ion releases of Run 1: 100% RH cell, and Run 2: H₂–air RH cycling cell.

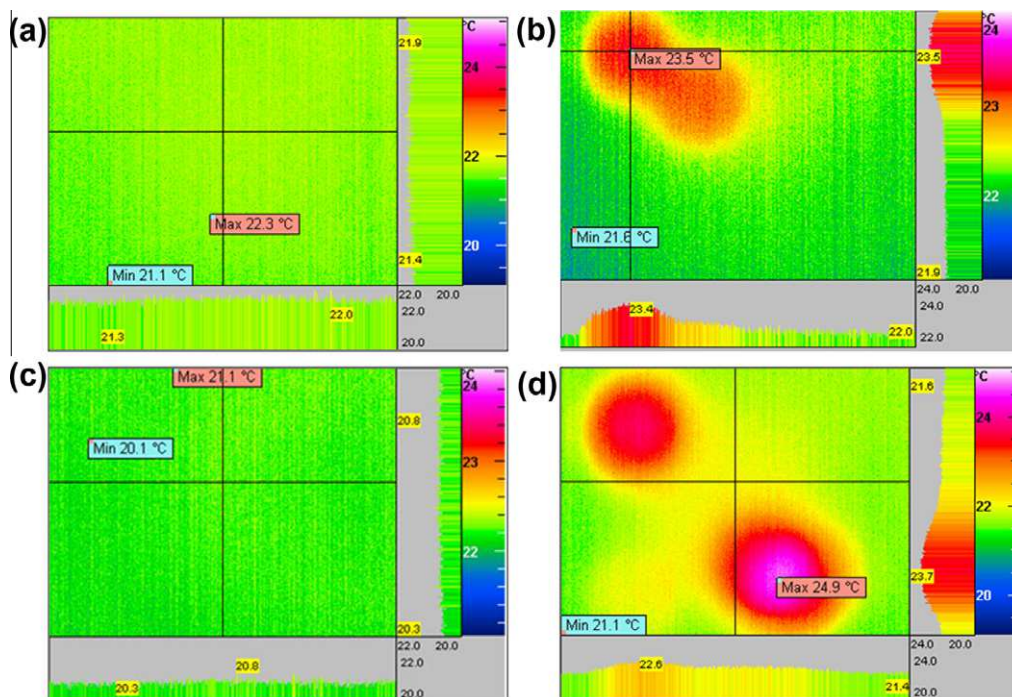


Fig. 7. IR camera images of Run 1 (100% RH cell): (a) fresh and (b) degraded MEAs at 650 h, and (c) fresh and (d) degraded MEAs at 840 h. Pure hydrogen and diluted hydrogen (20% H_2 in N_2) were respectively used for the MEAs at 650 h and at 840 h. The hydrogen was flowed in the anode inlet of the MEAs at 5 psi and 30 ml min^{-1} .

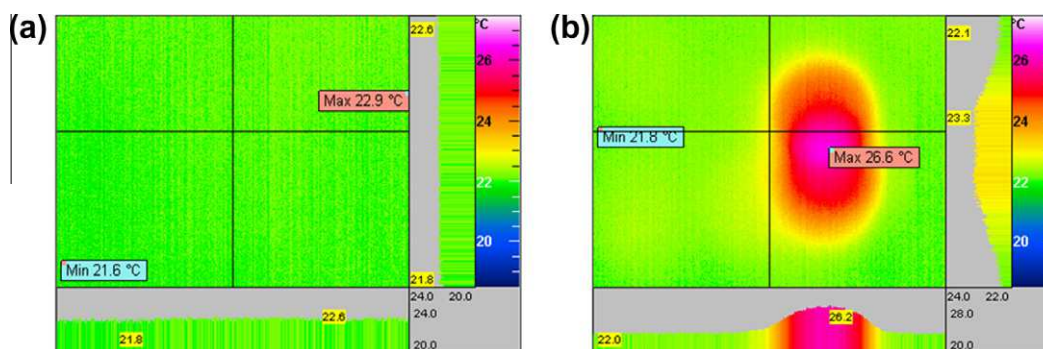


Fig. 8. IR camera images of Run 2 (RH cycling cell): (a) fresh and (b) degraded MEAs at 622 h. Diluted hydrogen (20% H_2 in N_2) was used by flowing in the anode inlet of the MEAs at 5 psi and 30 ml min^{-1} .

to the cathode inlet region. Also, there is a uniform MEA degradation throughout the sample (yellow¹ color distribution) starting at cathode outlet and latterly happening at cathode inlet. The uniform degradation is thought to lead to membrane thinning during the idle condition accelerated degradation test.

For the H_2 –air RH cycling cell, the IR imaging was conducted using 20% diluted H_2 in N_2 with 5 psi and 30 ml min^{-1} under the same conditions as Run 1. After 130 complete cycles, one big hot spot or pin-hole formation appeared close to anode and cathode inlets where dry/humidified reactants alternately enter as shown in Fig. 8b. Comparing with the fully humidified cell, the RH cycling cell differentiates pinhole formation of the shorter operating time without obviously showing the uniform MEA degradation throughout the sample. In other words, there is a smaller rate of membrane thinning than Run 1. This can also be confirmed by the SEM images.

As the results, the RH cycling cell displays higher maximum temperature distribution with the shorter operating time than the humidified cell. Change in RH is thus believed to have effect on the temperature distribution of the MEA due to the increase in reactant crossover, hot spot, and pin-hole formations.

3.5. RH effect as observed by scanning electron microscopy (SEM) imaging

After operated for 840 h (Run 1: 100% RH) and 622 h (Run 2: H_2 –air RH cycling), the MEAs were removed from the fuel cell hardware. Then, the membranes were separated off the GDL using liquid nitrogen. Overall, there is no visible rips or tears on the membranes for both Runs.

SEM images were taken for measuring the thickness and observing the morphology changes of the membranes. Fig. 9 shows the cross-sectional layers of fresh Gore™ 57 CCM consisting of cathode/anode catalyst layers, ePTFE reinforcement layer, and cathode/anode electrolyte layers. The overall thickness of the fresh membrane is 50 μm .

¹ For interpretation of color in Fig. 7, the reader is referred to the web version of this article.

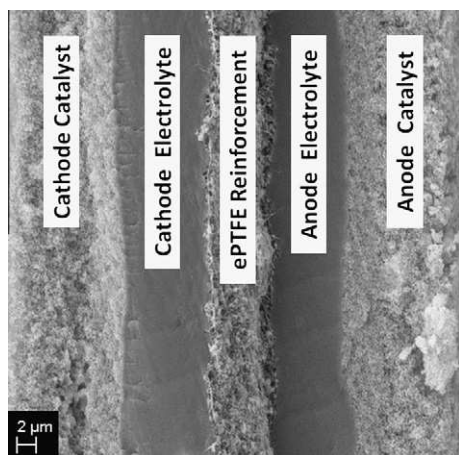


Fig. 9. SEM cross-sectional layers of a fresh Gore™ 57 CCM with 50 μm thickness (5000 \times magnification).

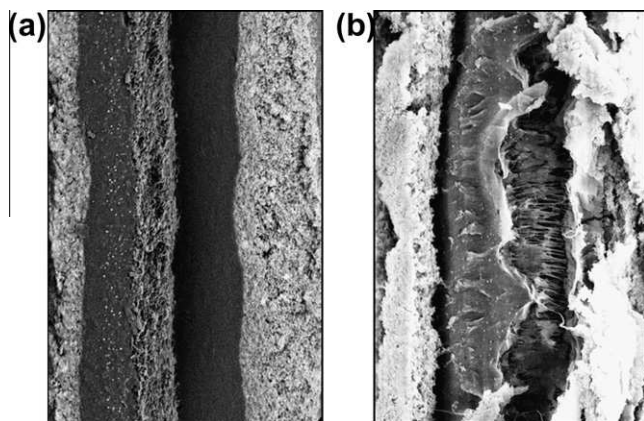


Fig. 10. SEM cross-sectional layers of (a) Run 1 with 27.5 μm thickness (5000 \times magnification) and (b) Run 2 with 34 μm thickness (5000 \times magnification) of Gore™ 57 CCMs.

Fig. 10a shows the cross-sectional layers of the CCM from Run 1. In this case, the overall thickness is reduced to 27.5 μm which is almost half of the original fresh CCM. Membrane thinning at the cathode side is clearly also observed for this humidified cell. The membrane thinning is a good method for observing membrane degradation since the degradation occurs when the membrane is consumed. Also, at the cathode electrolyte layer, there is an appearance of Pt band. The Pt band is believed to accelerate H_2O_2 production and enhance the membrane decomposition [28,29].

For Run 2, thinning of the membrane is also observed from the cross-sectional layers; however, the thickness of the reactant RH cycling membrane is reduced not as much as the humidified cell. Note that this MEA was operated about 25% less gross time. As there was simply less time to thin the MEA, the CCM thickness is reduced to 34 μm . Importantly, the RH cycled cell shows there is a crack of the catalyst layers combined with a fusion of the membrane and the electrode as can be seen from Fig. 10b. The fusion of the polymeric membrane and the electrolyte layers are believed to be caused by an increase of heat inside the cell during dry conditions, as well as stresses from membrane swelling/contraction during the RH cycling. The heat generated could melt the membrane and the electrode layers along with the stresses generated might later cause catalyst/membrane delamination. The delamination between the catalyst and the electrolyte membrane at the cathode side can be observed via the SEM images. The RH cycling is thus

thought to be a major cause of the mechanical failure in the fuel cell system.

4. Conclusions

Since it is impractical and costly to run full lifetime fuel cell tests, accelerated durability tests were used to observe the effect of RH on PEM fuel cell performance. This testing method was an alternative to longer term and more costly durability testing. The performance of a 100% RH humidified cell (Run 1) was compared with that of a RH cycling cell (Run 2). The results showed that the cell voltage degradation rates were 0.18 mV h^{-1} (Run 1) and 0.24 mV h^{-1} (Run 2). LSV was performed to diagnose the hydrogen crossover current of both cells. Run 2 clearly had a higher crossover current than Run 1; the crossover current of Run 2 rapidly increased and exceeded 10 mA cm^{-2} , defined as the point of membrane failure at approximately 450 h of operation as indicated by a sharp rise in crossover current, and an increase in the degradation rate. This diagnostic feature has been correlated with other observations as to indicate mechanical failure of the membrane, and pinhole formation. This failure is predictive of complete failure the cell in the near future. Ion chromatography also showed that Run 2 had a high fluoride ion release concentration, arising from degradation of the membrane structure. Note that there was no sharp change in the fluoride release rate indicating that this diagnostic was not representative of the sudden integrity failure, although the rate was generally higher during this test. In addition, the results from IR and SEM images showed that the RH cycling enhanced hot spot/pinhole formations, membrane thinning as well as stresses on the membrane. Overall, variation in RH is equivalent to mechanical load and it is believed to be a driving force that accelerates membrane mechanical failure in the fuel cell system.

Acknowledgment

The authors acknowledge the NRC-Helmholtz Joint Research Program and NSERC for their financial support.

References

- [1] Larminie J, Dicks A. Fuel cell systems explained. 2nd ed. Chichester, England: Wiley; 2003.
- [2] Barbir F. PEM fuel cells. London: Springer; 2006.
- [3] Collier A, Wang H, Yuan XZ, Zhang J, Wilkinson DP. Degradation of polymer electrolyte membranes. *Int J Hydrogen Energy* 2006;31(13):1838–54.
- [4] Healy J, Hayden C, Xie T, Olson K, Waldo R, Brundge M, et al. Aspects of the chemical degradation of PFSA ionomers used in PEM fuel cells. *Fuel Cells* 2005;5(2):302–8.
- [5] Pourcelly G, Oikonomou A, Gavach C. Influence of water content on the kinetics of counter-ion transport in perfluorosulphonic membranes. *J Electroanal Chem* 1990;287(1):43–59.
- [6] Zhang J, Tang Y, Song C, Xia Z, Li H, Wang H, et al. PEM fuel cell relative humidity (RH) and its effect on performance at high temperatures. *Electrochim Acta* 2008;53(16):5315–21.
- [7] Yang B, Fu Y, Manthiram A. Operation of thin Nafion-based self-humidifying membranes in proton exchange membrane fuel cells with dry O_2 and H_2 . *J Power Sources* 2005;139(1–2):170–5.
- [8] Uchida H, Ueno Y, Hagihara H, Watanabe M. Self-humidifying electrolyte membranes for fuel cells: preparation of highly dispersed TiO_2 particles in Nafion 112. *J Electrochem Soc* 2003;150(1):A57–62.
- [9] Endoh E, Terazono S, Widjaja H, Takimoto Y. Degradation study of MEA for PEMFCs under low humidity conditions. *Electrochem Solid-State Lett* 2004;7(7):A209–11.
- [10] Chiou JS, Paul DR. Gas permeation in a dry Nafion membrane. *Ind Chem Eng Res* 1988;27(11):2161–4.
- [11] Buchit FN, Srinivasa S. Operating proton exchange membrane fuel cells without external humidification of the reactant gases. *J Electrochem Soc* 1997;144(8):2767–72.
- [12] Williams MV, Kunz HR, Fenton JM. Operation of Nafion-based PEM fuel cells with no external humidification: influence of operating conditions and gas diffusion layers. *J Power Sources* 2004;135(1–2):122–34.

- [13] St-Pierre J, Wilkinson DP, Knights S, Bos M. Relationships between water management, contamination and lifetime degradation in PEFC. *J New Mater Electrochem Syst* 2000;3:99–106.
- [14] Kundu S, Simon LC, Fowler M, Grot S. Mechanical properties of Nafion™ electrolyte membranes under hydrated conditions. *Polymer* 2005;46(25): 11707–15.
- [15] Gu T, Lee WK, Vanzee JW. Quantifying the 'reverse water gas shift' reaction inside a PEM fuel cell. *Appl Catal B* 2005;56(1–2):43–9.
- [16] Okada T, Xie G, Tanabe Y. Theory of water management at the anode side of polymer electrolyte fuel cell membranes. *J Electroanal Chem* 1996;413(1–2):49–65.
- [17] Kundu S, Fowler M, Simon LC, Abouatallah R. Reversible and irreversible degradation in fuel cells during open circuit voltage durability testing. *J Power Sources* 2008;182(1):254–8.
- [18] Ma C, Zhang L, Mukerjee S, Ofer D, Nair B. An investigation of proton conduction in select PEM's and reaction layer interfaces designed for elevated temperature operation. *J Membr Sci* 2003;219(1–2):123–36.
- [19] Yu J, Matsuura T, Yoshikawa Y, Islam MN, Hori M. In situ analysis of performance degradation of a PEMFC under nonsaturated humidification. *Electrochem Solid-State Lett* 2005;8(3):A156–8.
- [20] Carrette L, Friedrich KA, Stimming U. Fuel cells: principles, types, fuels, and applications. *ChemPhysChem* 2000;1(4):163–93.
- [21] Inaba M, Kinumoto T, Kiriake M, Umebayashi R, Tasaka A, Ogumi Z. Gas crossover and membrane degradation in polymer electrolyte fuel cells. *Electrochim Acta* 2006;51(26):5746–53.
- [22] Ohma A, Suga S, Yamamoto S, Shinohara K. Membrane degradation behavior during open-circuit voltage hold test. *J Electrochem Soc* 2007;154(8): B757–60.
- [23] Kundu S, Karan K, Fowler M, Simon LC, Peppley B, Halliop E. Influence of micro-porous layer and operating conditions on the fluoride release rate and degradation of PEMFC membrane electrode assemblies. *J Power Sources* 2008;179(2):693–9.
- [24] Healy J, Hayden C, Xie T, Olson K, Waldo R, Brundage M, et al. *Fuel Cells* 2005;5(2):302–8.
- [25] Wayne RJ. Durability studies on polymer electrolyte membrane fuel cells. Case Western Reserve University; 2004.
- [26] Liu W, Ruth K, Rusch G. Membrane durability in PEM fuel cells. *J New Mater Electrochem Syst* 2001;4:227–31.
- [27] Yuan XZ, Zhang S, Wu J, Sun C, Wang H. Post analysis on MEA degradation: IR imaging, controlled technical report 2010; National Research Council Canada.
- [28] Huang C, Liu ZS, Mu DQ. The mechanical changes in the MEA of PEM fuel cells due to load cycling. *ECS Trans* 2008;16(2):1987–96.
- [29] Solasi R, Zou Y, Huang X, Reifsnider K, Condit D. On mechanical behavior and in-plane modeling of constrained PEM fuel cell membranes subjected to hydration and temperature cycles. *J Power Sources* 2007;167(2):366–77.